AIAA JOURNAL
Vol. 36, No. 9, September 1998

Self-Consistent Modeling of Volume and Surface Processes in Air Plasma

B. F. Gordiets* and C. M. Ferreira†
Instituto Superior Técnico, 1096 Lisbon, Portugal

A self-consistent model for bulk and surface kinetic processes in low-pressure flowing discharges in N_2–O_2 mixtures is presented. The model has a small number of input parameters and includes a large number of physical–chemical reactions that enable one to determine the concentrations of the different neutral (including NO and NO_2) and ionic species, as well as the populations of excited N_2, O_2, N, and O electronic states and N_2 vibrational levels, the density N_e of free electrons, their average kinetic energy and transport properties, the electric field, the average (across the tube) gas temperature, and the wall temperature. The kinetic model for surface processes, which is coupled to that for the bulk plasma, takes into account the processes of physical and chemical adsorption and desorption of N and O atoms, surface diffusion of these atoms, and surface chemical reactions leading to the formation of gas-phase N_2, O_2, NO, and NO_2 molecules. The probabilities for surface losses of N, O, and NO and the rates for surface production of gas-phase NO and NO_2 molecules have been obtained as a function of the surface temperature and the fluxes of gas-phase N and O atoms and NO molecules to the surface.

I. Introduction

THE nonequilibrium kinetics of low-pressure plasmas in nitrogen, oxygen, and their mixtures is an important field of research to improve our understanding of the processes occurring in the atmosphere and the ionosphere, as well as in a variety of modern plasma technologies. In particular, the knowledge of the volume and the surface kinetics of active species such as N and O atoms, $N(^2D)$, $O_2(a^1\Delta)$, and $N_2(A^3\Sigma)$ metastables, and NO molecules is important in understanding the workings of plasma reactors used for chemical synthesis, air pollution cleaning, or surface treatments of various materials. Such knowledge can also be important in understanding the re-entry heating of the Space Shuttle (surface recombination of O and N atoms) and the emissions near the surface of space vehicles in stationary orbits (surface production of gas-phase NO and NO_2 excited molecules).

The interaction of different atomic and molecular species with walls (including N and O atoms) in low-temperature plasmas can strongly influence the gas-phase concentrations of these species. Experimental data on the wall loss probabilities γ_N and γ_O for silica-based surfaces (see, for example, Refs. 1–5 and the literature cited therein) are usually used for plasma modeling. These probabilities are obtained, as a rule, from experiments with pure gases and measurements in postdischarges and are usually assumed to depend only on the surface temperature. Most theories developed so far to explain experimental temperature dependencies of γ_M (usually non-Arrhenius in a wide temperature range) take into consideration only one kind of atom.[1–5] Only in Refs. 6 and 7 have calculations for surface recombination of two kind of atoms (N and O) been made. However, surface diffusion processes of physisorbed atoms, which are important for relatively low wall temperatures, were not taken into consideration in Refs. 6 and 7.

To date many experimental results have been gathered showing that the interaction with surfaces of different atoms and molecules in gas mixtures N_2–N–O_2–O can significantly influence γ_N and γ_O and lead to the production of gas-phase heteronuclear molecules. For instance, optical and mass spectrometric measurements in space experiments[8,9] show that gas-phase NO_2 molecules can be produced on the Space Shuttle surface in the ram direction in stationary orbits, where strong interaction with the surface takes place for ramming O atoms and N_2 molecules. Laboratory measurements[10,11] for low-pressure (~1–2-torr) O_2 or N_2 low-temperature plasmas show a decrease in γ_O and γ_N with the addition of a small admixture (~1%) of the other gas (N_2 or O_2, respectively) in the discharge. A strong increase in γ_N, up to $\sim 10^{-2}$ as compared to values $\sim 10^{-4}$ for pure nitrogen, have been found in Ref. 12 for discharge in N_2–O_2 mixtures with relative O_2 concentration $\geq 20\%$. The interpretation of the Ref. 8–12 experiments requires the development of a kinetic theory for surface processes taking into account different kinds of atoms and surface diffusion of physisorbed atoms. Moreover, because of experimental evidence for the dependence of the probabilities γ_M on the relative concentrations of different kinds of gas-phase atoms, the development of a self-consistent model for gas-phase and surface kinetic processes in low-pressure nonequilibrium plasma becomes important and necessary. Such a model for low-pressure N_2–O_2 flowing discharges has been formulated for the first time in Refs. 12 and 13.

The aim of the present work is to extend our previous model[12,13] to include the kinetics of NO_2, NO_3, and N_2O_5 molecules and to account for surface processes that produce NO_2 gas-phase molecules. The latter processes are especially important for the interpretation of Space Shuttle experiments.[8,9]

II. Kinetic Model for Bulk Plasma Processes

Our model is one dimensional and self-consistent and applies to a dc flowing glow discharge and postdischarge. The input parameters of the model are the following: pressure p (in torr), radius R (in centimeter), and length L (in centimeter) of the discharge tube, electric current I (in milliampere), gas-flow rate Q [standard cubic centimeter per minute (sccm)], and initial gas temperature and composition, i.e., the relative oxygen concentration $X(\%)$ in the binary mixture $N_2 + X(\%)O_2$ at the entrance of gas into the discharge zone. The model gives the possibility to calculate, as a function of the axial coordinate z, the following properties of the bulk plasma: concentrations of N_2, O_2, NO, N_2O, NO_2, NO_3, N_2O_5, and O_3 molecules and N and O atoms in the ground electronic states; the populations of electronically excited states $N_2(A^3\Sigma_u^+, B^3\Pi_g, a'^1\Sigma_u^-, a^1\Pi_g, C^3\Pi_u, a''^1\Sigma_g^+)$, $O_2(a^1\Delta_g, b^1\Sigma_g^+)$, $N(^2D, ^2P)$, and $O(^1D, ^1S)$; concentration of ions N_2^+, $N_2^+(B)$, N_4^+, O^+, O_2^+, NO^+, and O^-; populations of vibrational levels of N_2 molecules in the ground electronic state $X^1\Sigma_g^+$, density N_e of free plasma electrons; their average kinetic $\frac{3}{2}kT_e$ and characteristic energy u_k (that is, the ratio of the free diffusion coefficient to the mobility); electron drift velocity v_d; electric

Presented as Paper 97-2504 at the AIAA 32nd Thermophysics Conference, Atlanta, GA, June 23–25, 1997; received Aug. 5, 1997; revision received May 11, 1998; accepted for publication May 24, 1998.

*Invited Scientist, Physics Department, Centro de Física de Plasmas; on leave from Lebedev Physical Institute of the Russian Academy of Sciences, Moscow 117924, Russia.

†Professor, Physics Department, Centro de Física de Plasmas.

field E responsible maintaining the discharge; average (across tube) gas temperature T; and temperature T_w of tube walls.

To determine these plasma properties, a coupled system of equations has been solved that describes the kinetics of free electrons, the vibrational kinetics of N_2 molecules, the kinetics of electronic states of molecules and atoms, the chemical kinetics of heavy neutrals and charged particles, the energy balance of the gas, and the charged particle balance determining the electric field needed to maintain the discharge. Empirical formulas have been derived and used for the calculation of the wall temperature T_w. Further, a set of equations for the surface kinetics of N and O atoms has been coupled to the gas-phase chemical kinetic equations, which renders our model fully self-consistent.

A. Kinetics of Free Electrons

The kinetics have been investigated using the quasistationary electron Boltzmann equation. The degree of ionization is assumed small in our case; therefore, electron–electron collisions were neglected. The collision integral, describing the collisions of electrons with heavy particles in the Boltzmann equation, also has been simplified. Because of the relatively small concentrations of the species involved, one can neglect electron collisions with excited electronic states of N_2, O_2, N, and O; vibrationally excited $O_2(v)$; and other neutral and ionic species. The sole exception to this concerns collisions with $N_2(X, v > 0)$ molecules, whose relative concentration can be large enough to affect the electron energy distribution function (EEDF). The EEDF is a solution of the Boltzmann equation, and the electron transport parameters and rate coefficients, as calculated from the obtained EEDF, are functions of the relative composition of the main gas components N_2 and O_2, reduced electric field E/N (where N is the total density of N_2 and O_2 molecules), and relative population of N_2 vibrational levels.

The electron cross sections used in the collision terms of the Boltzmann equation are the same as used in Ref. 14 for N_2 and in Ref. 15 for O_2. The reader should refer to these works for details.

B. Vibrational Kinetics

The populations of $N_2(X, v)$ vibrational levels have been determined from the usual coupled system of master equations taking into account 1) vibrational excitation and deexcitation by electron collisions (e–V processes); 2) vibration–vibration (V–V) energy exchanges; 3) vibrational exchanges between N_2 and O_2, NO molecules (V–V′ processes); 4) vibration–translation (V–T) energy exchanges in collisions $N_2(v)$ with N_2, O_2, NO, N, and O; 5) chemical reactions involving vibrationally excited N_2 molecules; and 6) one-quantum energy exchange in collisions of $N_2(v)$ with the wall. A list of these processes and the corresponding rate coefficients are given in Ref. 13.

Multiquanta V–T processes in N_2–N collisions play an important role in the populations of the upper vibrational levels. However, these processes were not included in the model.[13] We have used a simple analytical approximation to describe the total rate coefficients $K(v)$ for transitions from vibrational level v to all lower levels $v - \Delta v$, $1 \le \Delta v \le v$, due to $N_2(v) + N$ collisions:

$$K(v) = \begin{cases} K_0 \exp[-(E_a/T) + (\beta E_v/T)] & \text{if} \quad \beta E_v \le E_a \\ K_0 & \text{if} \quad \beta E_v \ge E_a \end{cases} \tag{1}$$

Here E_v is the vibrational energy of level v (in degrees Kelvin), and K_0, E_a, and β are parameters. Note that formula (1) sometimes is used for chemically active interactions of atoms with vibrationally excited molecules when such interactions have an energy barrier.[16] In Eq. (1), E_a is the energy of this barrier, and $\beta \le 1$ is a multiplier associated with a possible decrease in the activation barrier due to the vibrational energy E_v.

The numerical results[17,18] show that the main channels of N_2–N V–T relaxation are the transitions to the lower five levels. This is why we have assumed for simplicity that multiquanta V–T transitions take place only to the lower five levels, with equal probabilities. The value $K_0 \simeq 4 \times 10^{-10}(T/300)^{0.5}$ (cm^3/s) has been assumed, and E_a and β have been obtained by fitting Eq. (1) to numerical calculations.[17,18] The best fitting was obtained for $E_a \simeq 7280$ K and $\beta \simeq 0.065$.

Note that N_2–N collisions are important only for the N_2 vibrational kinetics in pure nitrogen. In N_2–O_2 mixtures, where O atoms are present in large amounts due to O_2 dissociation, the most important reaction affecting the N_2 upper-vibrational-level populations is the process

$$N_2(v \ge 12) + O \rightarrow NO + N \tag{2}$$

Reaction (2) is also very important for the production of NO. Here we have used the expression given in Ref. 19 for the rate coefficient of process (2). This expression is similar to Eq. (1), with $E_a \simeq 38{,}000$ K, $\beta \simeq 1$, and $K_0 \simeq 10^{-10}$ cm^3 s^{-1}. These values of E_a and K_0 correspond, respectively, to the activation energy and the preexponential factor of the rate coefficient for the classic reaction $O + N_2 \rightarrow NO + N$ without vibrational excitation of N_2. Note that, due to process (2), the N_2 vibrational distribution function is strongly depleted for the levels $v \ge 12$ in N_2–O_2 discharges with $\ge 1\%$ of $[O_2]$ (Ref. 13). For $v < 12$, this distribution is a Treanor-like distribution with a plateau.[16]

C. Kinetics of Electronic States and Chemical Kinetics

A large number of chemical reactions involving atoms, molecules, and ions and processes for excitation and deactivation of N_2 and O_2 electronic states are used in the present work. A list of the major processes with the corresponding rate coefficients is given in Ref. 13. In Table 1 are listed only those processes that have been ignored in the previous model[13] (that is, R1–R3, R9, R10, and R12–R27) and those used here with new rate coefficients.

Note that the new rate coefficient (from Ref. 20) for process R11 is very large compared to that used in Ref. 13, which now results in much smaller populations of $N_2(a'')$ metastables in discharge and postdischarge. As a result, the ionization processes from this state become much less effective than previously predicted.

Here we have added the fast processes R9 and R10 because the $N_2(a^1\Pi_g)$ and $N_2(a'^1\Sigma_u^-)$ singlet states are strongly coupled in the discharge.[21] The processes R3 and R12–R27 were added to describe volume production and losses of NO_2 molecules (see Table 1) (Refs. 20 and 22–29).

Note also that we have ignored in the present model the excitation of the electronic states $N_2(A, B, a'')$ upon collisions between two vibrationally excited $N_2(X)$ molecules. This differs from Ref. 13, but such processes are not very important under discharge conditions. We have found that neglecting such processes yields more accurate calculated populations of these states in postdischarge.

D. Interaction with the Wall

The interaction with the tube wall has a great effect for some species in low-pressure discharges. This interaction is approximately described using radially averaged rate coefficients for losses on the wall, ν_w, in our one-dimensional model:

$$\nu_w(s^{-1}) \approx [(R^2/5.8\mathcal{D}) + (2R/\gamma\bar{v})]^{-1} \tag{3}$$

where $\mathcal{D}$ is the diffusion coefficient (in square centimeters per second), R is the tube radius (in centimeters), $\bar{v}$ is the particle average velocity (near the wall), and γ is the wall deactivation probability (fraction of wall collisions leading to destruction of the species).

According to experimental evidence, the wall loss probabilities for the species

$$N_2(A), \qquad N(^2D), \qquad N(^2P), \qquad O(^1D), \qquad O(^1S) \tag{4}$$

are quite high (large γ values). For the pressures of interest, the wall loss rates of the species $N_2(A)$, $N(^2D)$, $N(^2P)$, $O(^1D)$, and $O(^1S)$, therefore, are determined by the corresponding rates of diffusion to the wall [first term on the right-hand side of Eq. (3)].[30,31] The diffusion coefficients have been taken from the literature. For the electronically excited particles, they have been assumed to be the same as for the corresponding ground state species. In the mixture N_2–O_2, the diffusion coefficients were calculated using the well-known Blanc's law. An effective ambipolar diffusion coefficient has been used for charged particles using the same procedure as in Ref. 32 to more accurately describe the transport at low pressures when the ion mean free path is not small compared to the tube radius.

Table 1 Volume processes and corresponding rate coefficients

Number	Process	Rate coefficients, ($cm^3\ s^{-1}$, 2 body) ($cm^6\ s^{-1}$, 3 body)	Reference
R1	$N_2(A) + N_2O \rightarrow N_2 + N + NO$	1×10^{-11}	22
R2	$N_2(A) + N_2O \rightarrow N_2 + N_2 + O$	1×10^{-11}	23
R3	$N_2(A) + NO_2 \rightarrow N_2 + NO + O$	1×10^{-12}	23
R4	$N_2(A) + N_2(v \geq 6) \rightarrow N_2(B) + N_2$	3×10^{-11}	24
R5	$N_2(B) + N_2 \rightarrow N_2(A) + N_2$	3×10^{-11}	24
R6	$N_2(B) + N_2 \rightarrow 2N_2$	2×10^{-12}	25
R7	$N_2(a') + N_2(A) \rightarrow N_4^+ + e$	4×10^{-12}	26
R8	$2N_2(v \geq 16) \rightarrow N_2(a') + N_2$	$2 \times 10^{-14} \exp(-700/T)$	26
R9	$N_2(a') + M \rightarrow N_2(a) + M$	$2 \times 10^{-11} \exp(-1{,}700/T)$	27
R10	$N_2(a) + M \rightarrow N_2(a') + M$	1×10^{-11}	27
R11	$N_2(a'') + N_2 \rightarrow 2N_2$	2.3×10^{-10}	20
R12	$N + NO_2 \rightarrow N_2 + O_2$	7×10^{-13}	28
R13	$N + NO_2 \rightarrow N_2 + O + O$	9×10^{-13}	28
R14	$N + NO_2 \rightarrow N_2O + O$	3×10^{-12}	28
R15	$N + NO_2 \rightarrow NO + NO$	2.3×10^{-12}	28
R16	$O + NO_2 \rightarrow NO + O_2$	$9.1 \times 10^{-12}(T/300)^{0.18}$	28
R17	$O + NO_3 \rightarrow NO_2 + O_2$	1×10^{-11}	28
R18	$O + N_2O_5 \rightarrow$ products	3×10^{-16}	28
R19	$NO + O_3 \rightarrow O_2 + NO_2$	$4.3 \times 10^{-12} \exp(-1{,}560/T)$	28
R20	$NO + NO_3 \rightarrow NO_2 + NO_2$	1.7×10^{-11}	28
R21	$NO_2 + O_3 \rightarrow O_2 + NO_3$	$1.2 \times 10^{-13} \exp(-2{,}450/T)$	28
R22	$NO_2 + NO_2 \rightarrow O_2 + NO + NO$	$3 \times 10^{-12} \exp(-13{,}540/T)$	28
R23	$NO_2 + NO_3 \rightarrow O_2 + NO + NO_2$	$2.3 \times 10^{-13} \exp(-1{,}600/T)$	28
R24	$NO_3 + NO_3 \rightarrow O_2 + NO_2 + NO_2$	$2.1 \times 10^{-11} \exp(-3{,}000/T)$	28
R25	$O + NO + M \rightarrow NO_2 + M$	$3 \times 10^{-33} \exp(940/T)$, $M = O_2$	29
——	——	$4.2 \times 10^{-33} \exp(940/T)$, $M = N_2$	29
R26	$O + NO_2 + M \rightarrow NO_3 + M$	$9 \times 10^{-32}(300/T)^2$	29
R27	$NO_2 + NO_3 + M \rightarrow N_2O_5 + M$	$3.7 \times 10^{-30}(300/T)^{4.1}$	23

As to the probabilities γ for one-quantum wall deactivation of $N_2(v)$ and deactivation of $N_2(a')$ metastables, we have used the values 4.5×10^{-4} (Ref. 33) and 10^{-3} (Ref. 26), respectively.

Wall recombination of N and O atoms is the main channel for losses of these species in low-pressure discharges. The probabilities γ_N and γ_O are small, with this being the main reason the corresponding loss rates are controlled by these probabilities rather than the diffusion time. The values γ_N and γ_O are modified in gas mixtures. This is why a kinetic model of surface processes involving N and O atoms has been developed to calculate γ_N, γ_O, γ_{NO}, and γ_{NO_2} in N_2–N–O_2–O mixtures. This is discussed in Sec. III.

E. Gas and Wall Temperatures

The radially averaged gas temperature has been calculated from the thermal balance equation, self-consistently with the vibrational and chemical kinetic equations. The most important sources of gas heating are V–T relaxation of N_2 and O_2 molecules, dissociation of N_2 and O_2 with production of hot N and O atoms, and deactivation of N_2 electronic states. Heating due to elastic electron collisions with heavy particles, excitation of N_2 and O_2 rotational levels (assuming fast rotational–translational relaxation), and exothermic chemical reactions have also been taken into account. Thermal conduction to the tube wall is the main gas-cooling mechanism. In our one-dimensional model, the power density lost by this process has been taken into account in the thermal balance equation by a term of the form $8\lambda(T - T_w)/R^2$, where T is the radially averaged gas temperature, T_w is the wall temperature, and λ is the thermal conductivity of the gas. This type of law results from assuming a parabolic gas temperature profile across the tube, with the temperature on the axis being given by $T_a = 2T - T_w$.

The wall temperature T_w is an important parameter as it influences the gas temperature and the rate coefficients of surface processes (see Sec. III). A fitting empirical formula for T_w was obtained in previous work[26] for a stationary discharge in a Pyrex® tube with radius $R \sim 1$ cm, for different pressures and electric currents, in the absence of forced external cooling of the tube walls. This formula was also used in the present model. It reads

$$T_w(K) = T_0 + C(EI)^\beta \tag{5}$$

where T_0 is the environment temperature; EI (in watt per centimeter) is the discharge power per unit length, where E (in volt per centimeter) is the electric field and I (in ampere) is the discharge electric current; and C and β are parameters. We have used the values $T_0 = 296$ K, $C = 82$, and $\beta = 0.87$.

The gas dynamics treatment in the present one-dimensional flowing discharge model is very simple and the same as in Ref. 13. The pressure was assumed constant along the tube axis z. This is a good approximation under our conditions of relatively small gas velocity, inasmuch as viscosity is, therefore, small, and the relaxation times for the gas temperature and the species concentrations are large as compared to the characteristic time for establishing the pressure along the tube, $\tau_p \simeq L/c_s$, where L is the length of the discharge tube and c_s the sound speed. The average gas velocity $v(z)$ has been determined from the conservation of the mass flow rate along the tube. The algorithm for numerically solving the coupled system of equations is also the same as in Ref. 13. The flowchart of this algorithm is displayed in Fig. 1 of Ref. 13.

Note that the equation for the electric field E has also been taken into consideration:

$$J = ev_d(E)N_e(E) \tag{6}$$

where J, e, v_d, and N_e are the current density, electron charge, drift velocity, and density of electrons. The drift velocity was calculated from the Boltzmann equation for the EEDF, and N_e was determined as the difference between the densities of positive and negative ions (that is, from the condition of plasma quasineutrality). Equation (6) is strongly nonlinear in E, due to the strong nonlinear dependence on E of the ionization rate coefficients determining the charged particle densities.

III. Kinetic Model for Surface Processes

As already mentioned, a kinetic model for surface processes was developed in the present work to calculate the surface losses of gas-phase N and O atoms and NO and NO_2 molecules and the surface production of gas-phase N_2, O_2, NO, and NO_2 molecules in discharges of binary molecular gas mixtures N_2–O_2. This model takes into account 1) physical adsorption and desorption of N and

Table 2 List of surface processes

Number	Process	Number	Process
S1	$N + F_v \rightleftharpoons N_f$	S11	$N + O_S \rightarrow (NO)_S$
S2	$O + F_v \rightleftharpoons O_f$	S12	$N_f + O_S \rightarrow (NO)_S + F$
S3	$N + S_v \rightleftharpoons N_S$	S13	$O + N_S \rightarrow (NO)_S$
S4	$N_f + S_v \rightarrow N_S + F_v$	S14	$O_f + N_S \rightarrow (NO)_S + F$
S5	$N + N_S \rightarrow N_2 + S_v$	S15	$NO + S_v \rightleftharpoons (NO)_S$
S6	$N_f + N_S \rightarrow N_2 + S_v + F_v$	S16	$NO_2 + S_v \rightleftharpoons (NO_2)_S$
S7	$O + S_v \rightleftharpoons O_S$	S17	$(NO)_S + O \rightarrow (NO_2)_S$
S8	$O_f + S_v \rightarrow O_S + F_v$	S18	$(NO)_S + O_f \rightarrow (NO_2)_S + F_v$
S9	$O + O_S \rightarrow O_2 + F_v + S_v$	S19	$NO + O_S \rightarrow (NO_2)_S$
S10	$O_f + O_S \rightarrow O_2 + S_v$		

O atoms, 2) chemical adsorption and desorption of both types of atoms and NO and NO_2 molecules at vacant chemically active sites on the surface, 3) surface diffusion of physisorbed N_f and O_f atoms, and 4) the reactions of chemisorbed N_S and O_S atoms both with gas-phase N and O atoms and NO molecules (Eley–Rideal mechanism) and with physisorbed N_f and O_f atoms (Langmuir–Hinshelwood mechanism), leading to the formation of gas-phase N_2 and O_2 and chemisorbed $(NO)_S$ and $(NO_2)_S$ molecules. $(NO)_S$ molecules can be desorbed or react with O and O_f and produce $(NO_2)_S$, which by desorption will produce gas-phase NO_2 molecules. The list of reactions taken into account is presented in Table 2. Herein, S_v and F_v denote vacant chemisorption (active) and physisorption sites, respectively.

Note that the present model for surface reactions is an extension of that reported in Ref. 12 for surface kinetics of N and O atoms in N_2–O_2 discharge. Taking only the first 15 reactions in Table 2 and assuming that the reverse reactions −S3 and −S7 are not efficient and that the reverse reaction −S15 is very fast, one obtains the list of reactions investigated in Ref. 12.

In the present model, reactions S16–S19 have been added to describe the surface production of NO_2, which is very important for understanding and interpreting Space Shuttle experiments on stationary orbits. Of course, the conditions for interaction of gas-phase atoms and molecules with a fast-moving Space Shuttle surface have some peculiarities (as compared to present laboratory conditions) that must be taken into account. We plan to investigate this in the future.

In spite of the increased number of reactions as compared to Ref. 12, the present model for surface kinetics remains simple and tractable. A number of processes, such as interactions between two physically adsorbed atoms or two chemically adsorbed particles, dissociative chemisorption of molecules, and processes involving physisorbed molecules, are discarded in this model. The neglect of dissociative chemisorption and reactions between two chemisorbed particles is justified under the present relatively low surface density of active sites (discussed subsequently) and low wall temperatures ($T_w \leq 1000$ K) due to the high energy threshold of such reactions. Note that a model accounting for surface diffusion of physisorbed atoms was investigated in Ref. 1 but ignoring the reactions of these atoms with vacant active sites and considering only atoms of a single kind. Only the two processes S5 and S6 from our list of reactions were taken into account in Ref. 1. A model with two different atoms (N and O) has been proposed in Refs. 6 and 7, but this was used only for interpretation of high-temperature experiments and did not include processes with NO_2, physisorbed atoms, and surface diffusion and reactions of these atoms, i.e., processes S1, S2, S4, S6, S8, S10, S12, S14, and S16–S19.

Note that the rate coefficients for processes involving gas-phase particles (S1–S3, S5, S7, S9, S11, S13, S15, S16, and S19 in Table 2) are in cubic centimeter second, reciprocal. The rate coefficients K_i for surface reactions ($i =$ S4, S6, S8, S10, S12, S14, and S18) are in units of square centimeter second, reciprocal. They are determined by surface diffusion coefficients D_N and D_O (in square centimeter second, reciprocal) for N_f and O_f physisorbed atoms:

$$K_i = D_M K_i^0 \exp(-E_i/T_w) \tag{7}$$

where K_i^0 are dimensionless steric factors (≤ 1) and E_i activation energies (in degree Kelvin) of the chemical processes i. The surface diffusion coefficients D_M can be expressed by the following formula[1]:

$$D_M \simeq \tfrac{1}{4} a^2 \nu_{DM}^0 \exp(-E_{DM}/T_w)$$
$$\simeq \left(\nu_{DM}^0 / 4[F]\right) \exp(-E_{DM}/T_w) \tag{8}$$

where a is an elementary distance for the jump of a physisorbed atom from one physisorption site to another (that is, the distance between neighboring sites), ν_{DM}^0 is the frequency factor, and E_{DM} is the activation energy for surface diffusion of M atoms.

The desorption coefficients K_{-S1} and K_{-S2} (in seconds, reciprocal) of N_f and O_f physisorbed atoms are

$$K_{-i} \simeq \nu_{dM}^0 \exp(-E_{dM}/T_w) \tag{9}$$

where ν_{dM}^0 is the frequency factor and E_{dM} is the activation energy for desorption of M atoms ($M =$ N for $i = 1$ and $M =$ O for $i = 2$). The coefficients of desorption for chemically adsorbed atoms and molecules (processes −S3, −S7, −S15, and −S16) have the same dimensions and form as Eq. (9) but with the pertinent frequency factors and activation energies for desorption.

From the master kinetic equations for processes S1–S19, with rate coefficients K_i, under steady-state conditions one readily obtains

$$[N_f] = A_N[N], \qquad [O_f] = A_O[O] \tag{10}$$

where

$$A_N = K_{S1}\tau_N[F_v], \qquad A_O = K_{S2}\tau_O[F_v] \tag{11}$$

$$[F_v] = \frac{[F]}{1 + K_{S1}\tau_N[N] + K_{S2}\tau_O[O]} \tag{12}$$

$$[N_S] = \alpha_N[S_v], \qquad [O_S] = \alpha_O[S_v] \tag{13}$$

$$[(NO)_S] = \alpha_{NO}[S_v], \qquad [(NO_2)_S] = \alpha_{NO_2}[S_v] \tag{14}$$

$$[S_v] = \frac{[S]}{1 + \sum_M \alpha_M} \tag{15}$$

with $M =$ N, O, NO, NO_2. The variables $[X]$ in Eqs. (10–15) are the volume or the surface densities of the X species, the values

$$\frac{\alpha_M}{1 + \sum_M \alpha_M}$$

are the coverages of chemically active sites by the species $M =$ O, N, NO, NO_2, and τ_N and τ_O are the lifetimes of physically adsorbed N_f and O_f atoms, respectively,

$$\tau_N = (K_{-S1} + K_4[S_v] + K_{S6}[N_S] + K_{S12}[O_S])^{-1} \tag{16}$$

$$\tau_O = (K_{-S2} + K_{S8}[S_v] + K_{S10}[O_S] + K_{S14}[N_S] + K_{S18}[(NO)_S])^{-1} \tag{17}$$

For a wide range of the concentrations [N] and [O] and for $T_w \geq 300$ K, we can further assume that

$$K_{S1}[N] \ll K_{-S4}, \qquad K_{S2}[O] \ll K_{-S2} \tag{18}$$

so that $[F_v] \simeq [F]$. This condition corresponds to a small coverage of the surface by physisorbed atoms. Under this assumption, using dimensionless rate coefficients, the α_M in Eqs. (13–15) can be expressed as

$$\alpha_N = \frac{(K'_{S3} + P_{S4})\Phi_N}{K'_{-S3} + (K'_{S5} + P_{S6})\Phi_N + (K'_{S13} + P_{S14})\Phi_O} \tag{19}$$

$$\alpha_O = \frac{(K'_{S7} + P_{S8})\Phi_O}{K'_{-S7} + (K'_{S9} + P_{S10})\Phi_O + (K'_{S11} + P_{S12})\Phi_N + K'_{S19}\Phi_{NO}} \tag{20}$$

$$\alpha_{NO} = \frac{(K'_{11} + P_{S12})\alpha_O \Phi_N + (K'_{S13} + P_{S14})\alpha_N \Phi_O + K'_{S15}\Phi_{NO}}{K'_{-S15} + (K'_{S17} + P_{S18})\Phi_O} \tag{21}$$

$$\alpha_{NO_2} = \frac{(K'_{S17} + P_{S18})\alpha_{NO}\Phi_O + K'_{S19}\alpha_O \Phi_{NO} + K'_{S16}\Phi_{NO_2}}{K'_{-S16}} \tag{22}$$

In Eqs. (19–22), Φ_M are the fluxes of gas-phase atoms or molecules $M = \mathrm{N}$, O, NO, $\mathrm{NO_2}$ to the surface, which in our case ($l \ll R$, where l is the atom mean free path) is

$$\Phi_M = \tfrac{1}{4}\overline{v_M}[M] \tag{23}$$

where $\overline{v_M}$ denotes the mean velocity of the gas-phase particle M near the surface. The rate coefficients K'_i and P_i are defined by the following formulas:

$$K'_i = \frac{4[S]}{\overline{v_M}}K_i, \qquad K'_j = \frac{4[F]}{\overline{v_M}}K_j, \qquad K'_n = [S]K_n \tag{24}$$

with $\overline{v_M} = \overline{v_N}$ for $j = \mathrm{S1}$, $i = \mathrm{S3}$, S5, S11; $\overline{v_M} = \overline{v_O}$ for $j = \mathrm{S2}$, $i = \mathrm{S7}$, S9, S13, S17; $\overline{v_M} = \overline{v_{NO}}$ for $i = \mathrm{S15}$, S19; $\overline{v_M} = \overline{v_{NO_2}}$ for $i = S16$; $n = -\mathrm{S3}, -\mathrm{S7}, -\mathrm{S15}, -\mathrm{S16}$; and

$$P_i = K'_j K_i \tau_M [S] \tag{25}$$

with $M = \mathrm{N}$ for $j = \mathrm{S1}$, $i = \mathrm{S4}$, S6, S12; $M = \mathrm{O}$ for $j = \mathrm{S2}$, $i = \mathrm{S8}$, S10, S14, S18. All of the coefficients K'_i and P_i except K'_{-S3}, K'_{-S7}, K'_{-S15}, and K'_{-S16} are dimensionless and represent the reaction probabilities. The units of K'_{-S3}, K'_{-S7}, K'_{-S15}, and K'_{-S16} are square centimeter, reciprocal, second, reciprocal. They are proportional to the chemical desorption fluxes.

It is appropriate to express the dimensionless reaction probabilities (24) for processes involving gas-phase atoms and molecules in the following form:

$$K'_i = ([S]/[F])K_i^0 \exp(-E_i/T_{gw}) \tag{26}$$

$$K'_j \equiv P_M = K_M^0 \exp\left(-E_M^0 \big/ T_{gw}\right) \tag{27}$$

where $i = \mathrm{S3}$, S5, S7, S9, S11, S13, S15, S16, S17, S19; $M = \mathrm{N}$ for $j = \mathrm{S1}$ and $M = \mathrm{O}$ for $j = \mathrm{S2}$. The values K'_i are the probabilities for gas-phase atoms or molecules to be chemically adsorbed (processes S3, S7, S15, and S16) or react with chemically adsorbed particles (processes S5, S9, S11, S13, S17, and S19). The ratio $[S]/[F]$ represents the probability of direct impingement of gas-phase particles on either vacant or occupied active sites; it is the fraction of the surface covered by such sites. The values $K'_j \equiv P_M$ are the probabilities for gas-phase atoms $M = \mathrm{N}$, O to be physically adsorbed (processes S1 and S2). The multipliers K_i^0 and K_M^0 in Eqs. (26) and (27) are the steric factors for surface processes, involving gas-phase particles. E_i is the activation energy of reaction i in absolute temperature units, E_M^0 is the activation energy for physical adsorption of M atoms, and T_{gw} is the gas temperature near the wall, which we will assume to be equal to the wall temperature T_w.

The values of P_i in Eq. (25) for surface processes, involving physisorbed N_f and O_f atoms ($i = \mathrm{S4}$, S6, S8, S10, S12, S14, S18), are determined by the following formulas:

$$P_i = P_M P_i^0 \times [1 + \Psi_M]^{-1} \tag{28}$$

$$P_i^0 = K_{Mi}\exp\left(\frac{E_{dM} - E_{DM} - E_i}{T_w}\right), \qquad K_{Mi} = \frac{1}{4}K_i^0 \frac{[S]}{[F]}\frac{\nu_{DM}^0}{\nu_{dM}^0} \tag{29}$$

$$\Psi_N = \delta\left(P_{S4}^0 + \alpha_N P_{S6}^0 + \alpha_O P_{S12}^0\right) \tag{30}$$

$$\Psi_O = \delta\left(P_{S8}^0 + \alpha_O P_{S10}^0 + \alpha_N P_{S14}^0 + \alpha_{NO} P_{S18}^0\right)$$

$$\delta = \frac{1}{1 + \sum_M \alpha_M} \tag{31}$$

(with $M = \mathrm{N}$, O, NO, $\mathrm{NO_2}$). Formulas (28–31) can be obtained from Eqs. (7–9), (16), (17), and (25). The factors Ψ_N and Ψ_O describe the influence on the lifetime of N_f and O_f physisorbed atoms of the surface chemical processes (in addition to desorption). Note that a mistake has been made in Ref. 12 in expressing such factors. However, for wall temperatures $T_w \geq 300$ K, the lifetime of physisorbed atoms is controlled by desorption. In this case, $\Psi_M \ll 1$, and these factors have no influence on the probabilities P_i.

Let us now find the wall loss probabilities γ_M. Note that the diffusion rates of gas-phase N and O atoms to the wall is much faster than the corresponding rates for wall destruction under typical low-pressure discharge conditions ($p \leq 5$ torr and $R \leq 2$ cm). [That is, the second term on the right-hand-side of Eq. (3) is the most important.] This is known from experimental data. The same will be assumed for NO and $\mathrm{NO_2}$ molecules, too. Under such condition, the net rates for wall loss and production of gas-phase N and O atoms and NO and $\mathrm{NO_2}$ molecules in infinite cylindrical geometry are the following:

$$\left(\frac{d[N]}{dt}\right)_{wall} = -\frac{2}{R}\epsilon\left\{\left(K_{S1}[F_v] - K_{-S1}\frac{[N_f]}{[N]} + K_{S3}[S_v] + K_{S5}[N_S] + K_{S11}[O_S]\right)[N] - K_{-S3}[N_S]\right\} \tag{32}$$

$$\left(\frac{d[O]}{dt}\right)_{wall} = -\frac{2}{R}\epsilon\left\{\left(K_{S2}[F_v] - K_{-S2}\frac{[O_f]}{[O]} + K_{S7}[S_v] + K_{S9}[O_S] + K_{S13}[N_S] + K_{S17}[(NO)_S]\right)[O] - K_{-S7}[O_S]\right\} \tag{33}$$

$$\left(\frac{d[NO]}{dt}\right)_{wall} = -\frac{2}{R}\epsilon\{(K_{S15}[S_v] + K_{S19}[O_S])[NO] - K_{-S15}[(NO)_S]\} \tag{34}$$

$$\left(\frac{d[NO_2]}{dt}\right)_{wall} = -\frac{2}{R}\epsilon\{K_{S16}[S_v][NO_2] - K_{-S16}[(NO_2)_S]\} \tag{35}$$

Herein, $\epsilon \geq 1$ is the roughness factor, that is, the ratio of the real surface area to the geometric surface area, per unit length.

Using Eqs. (10–17) and (19–22), Eqs. (32–35) can be rewritten in the form

$$\left(\frac{d[N]}{dt}\right)_{wall} = -\frac{\overline{v_N}}{2R}\gamma_N[N] + \frac{2}{R}K'_{-S3}\epsilon\delta\alpha_N \tag{36}$$

$$\left(\frac{d[O]}{dt}\right)_{wall} = -\frac{\overline{v_O}}{2R}\gamma_O[O] + \frac{2}{R}K'_{-S7}\epsilon\delta\alpha_O \tag{37}$$

$$\left(\frac{d[NO]}{dt}\right)_{wall} = -\frac{\overline{v_{NO}}}{2R}\gamma_{NO}[NO] + \frac{2}{R}K'_{-S15}\epsilon\delta\alpha_{NO} \tag{38}$$

$$\left(\frac{d[NO_2]}{dt}\right)_{wall} = -\frac{\overline{v_{NO_2}}}{2R}\gamma_{NO_2}[NO_2] + \frac{2}{R}K'_{-S16}\epsilon\delta\alpha_{NO_2} \tag{39}$$

where γ_M is the probability for wall losses given by the expression

$$\gamma_N = \gamma_N^{(1)} + \gamma_N^{(2)} \tag{40}$$

$$\gamma_N^{(1)} = \epsilon\delta(K'_{S3} + K'_{S5}\alpha_N + P_{S4} + P_{S6}\alpha_N) \tag{41}$$

$$\gamma_N^{(2)} = \epsilon\delta(K'_{S11} + P_{S12})\alpha_O \tag{42}$$

$$\gamma_O = \gamma_O^{(1)} + \gamma_O^{(2)} + \gamma_O^{(3)} \tag{43}$$

$$\gamma_O^{(1)} = \epsilon\delta(K'_{S7} + K'_{S9}\alpha_O + P_{S8} + P_{S10}\alpha_O) \tag{44}$$

$$\gamma_O^{(2)} = \epsilon\delta(K'_{S13} + P_{S14})\alpha_N \tag{45}$$

$$\gamma_O^{(3)} = \epsilon\delta(K'_{S17} + P_{S18})\alpha_{NO} \tag{46}$$

$$\gamma_{NO} = \epsilon\delta(K'_{S15} + K'_{S19}\alpha_O) \tag{47}$$

$$\gamma_{NO_2} = \epsilon\delta K'_{S16} \tag{48}$$

Note that $\gamma_N^{(1)}$ and $\gamma_O^{(1)}$ are responsible for the production of, respectively, $\mathrm{N_2}$ and $\mathrm{O_2}$ gas-phase molecules, and $\gamma_N^{(2)}$ and $\gamma_O^{(2)}$ for the production of $(\mathrm{NO})_S$.

In principle, formulas (36–48) enable one to calculate the wall loss and production of gas-phase atoms and molecules N, O, NO, and NO_2. Of course, in practice the use of these formulas presents difficulties due to the lack of information about rate coefficients and other parameters of the model. Some important parameters can be estimated, but it is clear that simplifications are necessary for practical purposes.

We will assume for the sake of simplicity that the following inequalities hold under discharge conditions:

$$(K'_{S17} + P_{S18})\Phi_O \gg (K'_{S11} + P_{S12})\Phi_N, \qquad (K_{S13'} + P_{S14})\Phi_O \qquad (49)$$
$$K'_{S15}\Phi_{NO}, \qquad K'_{-S15}$$

$$K'_{S19}\Phi_{NO} \ll (K'_{S9} + P_{S10})\Phi_O, \qquad (K'_{S11} + P_{S12})\Phi_N \qquad (50)$$

For conditions (49) and (50) we have $\alpha_{NO}, \alpha_{NO_2} \ll \alpha_N$, and α_O. That is, the fractions of chemically active sites occupied by $(NO)_S$ and $(NO_2)_S$ molecules are small as compared to those occupied by N_S and O_S.

Using inequalities (49) and (50), it can be derived from Eqs. (19–22) and (40–48) that $(NO)_S$ and $(NO_2)_S$ have a weak influence on γ_O and γ_N. The main loss channels for these species are the reactions S17 and S18 and the reverse reactions −S15 and −S16, with production of gas-phase NO and NO_2. These circumstances simplify the analysis of surface kinetics.

IV. Calculations and Discussion

As a test of the model for bulk processes, the electric field E in N_2 dc glow discharge without gas flow has been calculated and compared with experimental data[31] (Fig. 1). Associative ionization of N_2 via process R7 and excitation of $N_2(a')$ via process R8 are important in determining the values of the discharge-sustainingfield E. Using the rate coefficients from Table 2 for processes R7–R10 and a probability $\gamma_{a'} \simeq 10^{-3}$ for wall losses of $N_2(a')$ yields reasonable agreement between theory and experiment in a wide range of currents ($I = 1$–100 mA) and pressures ($p = 0.2$–2 torr).

It is interesting to compare model calculations and experimental measurements of different plasma properties for N_2–O_2 mixtures. Detailed measurements have been carried out[13,34] for a low-pressure glow N_2–O_2 discharge, with O_2 percentages $X_{O_2} = 0$–100%, of the gas temperature T, N_2 vibrational temperature, electron density N_e, electric field E, relative populations of $N_2(A)$, $N_2(C)$, and $N_2^+(B)$, concentration of N atoms (for $X_{O_2} \leq 10\%$), and concentrations of O and NO. Measurements and calculations from our kinetic model[13] are in reasonable agreement.

Note that, for [O] and [NO], such an agreement could be achieved only using values of γ_O and γ_N much different from those obtained from afterglow experiments.[1–5] The values of γ_O and γ_N under discharge conditions can be obtained from a comparison between theoretical and experimental O and NO concentrations under different discharge conditions. (Note that [NO] is controlled by the fast reaction $NO + N \rightarrow N_2 + O$; therefore, it depends on [N] and γ_N.) Such comparisons were made in Ref. 12 and 34–37 for pure O_2 discharges and in Ref. 12 for N_2–O_2 mixtures. The results[12] for γ_O obtained are presented in Fig. 2 (symbols).

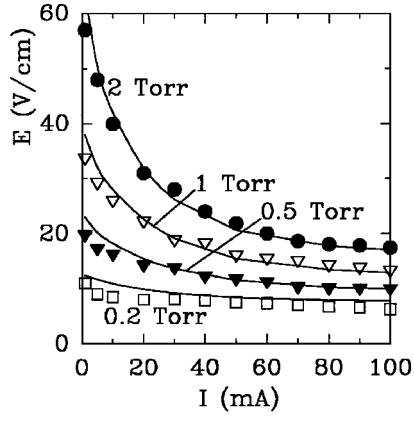

Fig. 1 Electric field E vs current I in a N_2 dc discharge without gas flow in a 1-cm-radius tube for different gas pressures: symbols, Ref. 31 measurements, and —, present calculations.

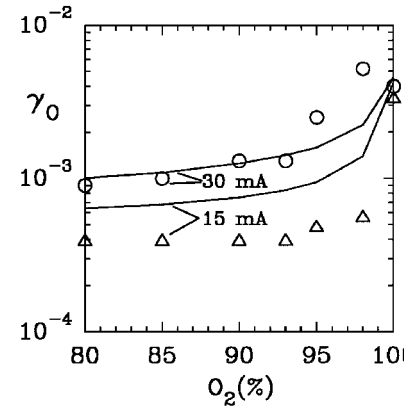

Fig. 2 Wall loss probability of O atoms in N_2–O_2 discharge vs O_2 percentage, for different currents, pressure 2 torr, gas flow rate 100 sccm, distance from gas entrance in discharge 43 cm: symbols, measurements from Ref. 12, and —, present calculations.

It can be seen from Fig. 2 that γ_O is relatively large and decreases with a small amount of N_2 admixed into a O_2 discharge. Such high γ_O values are required to interpret experimental O atom densities in discharges. Similarly, high γ_N values in N_2–O_2 discharges, with $X_{O_2} \geq 20\%$, are necessary to explain the observed NO densities. Note, however, that much smaller γ_O and γ_N values have been derived from experiments in pure gases and afterglows.[1–5]

To solve this apparent paradox and explain experiments,[12,34–37] it is reasonable to assume that additional chemically active sites exist on the wall under discharge conditions. Such an assumption was made in Ref. 12, and the parameters determining γ_O and γ_N in formulas (40–46) have been estimated, for relatively low wall temperatures $T_w \leq 400$ K, when surface diffusion and reactions of physisorbed N_f and O_f atoms control the surface losses of gas-phase N and O atoms. Here, however, we have to correct the results in Ref. 12 because of the Ψ_M factor. This factor affects the fitting values of the parameters $E_{dO} - E_{DO} - E_O^0$ and $K_O^0 K_{Oi}$ involved in the determination of γ_O [see Eqs. (27–31) and (43–46)]. (It was assumed in Ref. 12 that $E_O^0 = 0$; $K_O^0 = 1$.) After such a correction, the new values obtained here read as follows: $E_{dO} - E_{DO} - E_O^0 \simeq 2000$ K and $K_O^0 K_{Oi} \simeq 1.5 \times 10^{-3}$ and 1.5×10^{-3}, respectively, for the first and the second systems of chemically active sites (with the same site numeration as in Ref. 12). These new values yield the results for γ_O shown in Fig. 2 (lines).

Calculations of O and NO concentrations taking into consideration either two systems of chemically active sites or only one single ordinary system (second system according to the designation adopted in Ref. 12) are shown in Figs. 3 and 4. It can be seen that the calculations with only one system do not agree with experiment.

The nature of the additional system of chemically active sites under discharge conditions is so far unclear. It could be connected with surface ions resulting from the discharge electron and ion fluxes to the surface. For example, the surface will likely be partly covered with negative atomic ions due to surface attachment of electrons to O_S atoms. If we assume that the lifetime τ_{ion} of surface ions is controlled by mutual ion–ion recombination, from the balance equation for the concentration $[S^{ion}]$ of surface ions

$$\Phi^{ion} = (1/\tau_{ion})[S^{ion}] \equiv K_{rec}^{ion}[S^{ion}]^2$$
$$\equiv (\nu_{ion}/4[F])\exp(-E_{ion}/T_w)[S^{ion}]^2 \qquad (51)$$

it is easy to obtain the following expression for the relative surface density of positive and negative charges:

$$\frac{[S^{ion}]}{[F]} \simeq 2\sqrt{a^2 \frac{\Phi^{ion}}{\nu_{ion}}}\exp\left(\frac{E_{ion}}{2T_w}\right) \qquad (52)$$

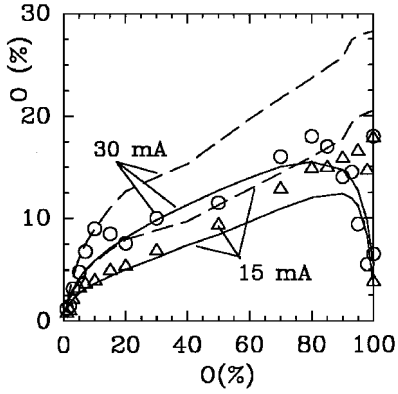

Fig. 3 Relative concentration of O atoms vs O_2 percentage in a N_2–O_2 dc discharge in 0.8-cm-radius tube for pressure 2 torr, gas flow rate 100 sccm at a distance of 43 cm from gas entrance into discharge: symbols, measurements from Refs. 12 and 13; —, present calculations; and – –, calculations using only the ordinary system of surface chemically active sites to determine γ_O.

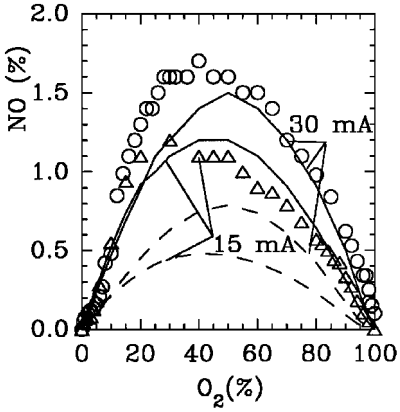

Fig. 4 Relative NO density vs O_2 percentage: symbols, measurements from Refs. 12 and 13; —, present calculations; and – –, calculations with small $\gamma_N \leq 10^{-4}$ with the ordinary system of surface chemically active sites. Discharge parameters are the same as in Fig. 3.

In Eqs. (51) and (52), K_{rec}^{ion} is the rate coefficient (in square centimeter per second) for surface ion–ion recombination; ν_{ion} and E_{ion} are the frequency factor (in seconds, reciprocal) and the activation energy (in degree Kelvin) for surface diffusion of charged particles; a is the elementary distance (in centimeter) for a jump of physisorbed ions; Φ_{ion} is the ambipolar diffusion flux (in square centimeter, reciprocal, second, reciprocal) of plasma electrons and ions to the surface, which is the source of surface ions. For the typical values $T_w \sim 350$ K, $\Phi^{ion} \sim 10^{14}$ cm^{-2} s^{-1} and physically acceptable values $a \sim 10^{-8}$ cm, $\nu_{ion} \sim 10^{13}$ s^{-1}, and $E_{ion} \sim 7500$ K, one can estimate from Eq. (52) that $[S^{ion}]/[F] \sim 10^{-3}$. This value corresponds to the order of magnitude of the relative density of chemically active sites $[S]/[F]$ estimated in Ref. 12 to explain the large γ_O and γ_N values measured under discharge conditions. Thus far, this explanation is just a working hypothesis that needs to be further worked out in the future.

Note that, in postdischarge, where free electrons are absent, the probabilities γ_O and γ_N are determined only by the ordinary single system of chemically active sites. In this case, the present model yields reasonable agreement with experimental data for silica-based surfaces using the values $E_{dO} - E_{DO} - E_O^0 \simeq 2000$ K; $K_O^0 K_{Oi} \simeq 1.5 \times 10^{-3}$ (for $i = S8, S10$), $E_{dN} - E_{DN} - E_N^0 \simeq 3100$ K; $K_N^0 K_{Ni} \simeq 1.5 \times 10^{-5}$ (for $i = S4, S6$), and $E_{S4} \simeq 900$ K, $E_{S6} \simeq 2400$ K, $E_{S8} \simeq 0$ K, $E_{S10} \simeq 3100$ K, $[S]/[F] \simeq 3 \times 10^{-3}$, and $\epsilon = 2.4$. A comparison is shown in Figs. 5 and 6 with experimental data from different authors.[1,38–48] These data are taken from Refs. 1 and 38–48, but values of γ_N smaller than 10^{-4} are not presented in Fig. 6.

Note that the calculations of γ_O and γ_N in Figs. 5 and 6 were carried out taking into account the reactions of chemisorbed atoms with both physisorbed atoms (Langmuir–Hinshelwood mechanism) and gas-phase atoms (Eley–Rideal mechanism). For the latter reactions (which are important for $T_w \geq 500$ K), we assumed that all steric factors are equal to 1 and the activation energies E_i are the same as for the reactions with physisorbed atoms. Taking into consideration both mechanisms allows one to explain the non-Arrhenius temperature dependencies of γ_O and γ_N over a wide temperature range, from ~300 up to ~2000 K. This can be seen particularly for γ_N in Fig. 6.

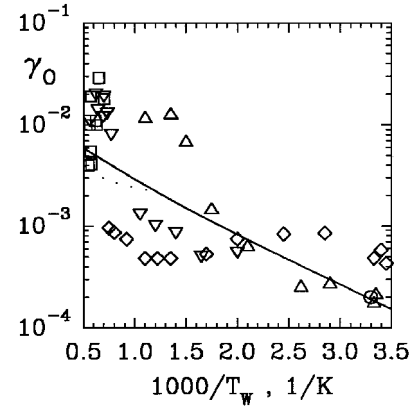

Fig. 5 Dependence of γ_O on the wall temperature: —, calculations from our model with the ordinary system of chemically active sites (post-discharge), and symbols, measurements from Ref. 38 (△), Ref. 39 (▽), Ref. 40 (□), Ref. 41 (○), Ref. 1 (◇), and Ref. 42 (· · ·).

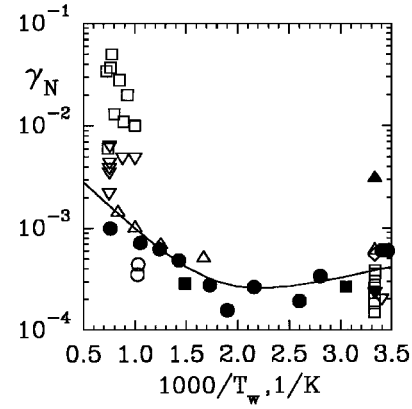

Fig. 6 Dependence of γ_N on the wall temperature: —, calculations from our model with ordinary system of chemically active sites (post-discharge), and symbols, measurements from Ref. 43 (□), Ref. 44 (△), Ref. 45 (▽), Ref. 46 (○), Ref. 47 (■), Ref. 48 (▲), Ref. 44 (▼), and Ref. 1 (●).

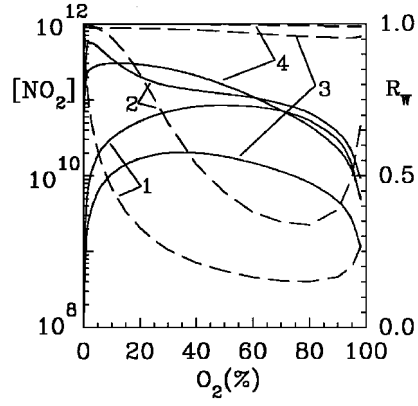

Fig. 7 Calculated NO_2 density (—) and relative rate R_w for surface production of NO_2 (– –) vs O_2 percentage, for the same conditions as in Fig. 3 but a fixed discharge current of 30 mA and pressures 2 torr (curves 1 and 2) and 0.2 torr (curves 3 and 4); the activation energy for desorption of chemically adsorbed $(NO)_S$ molecules is assumed to be 5000 K (curves 1 and 3) or 10,000 K (curves 2 and 4).

Calculated densities of gas-phase NO_2 molecules are given in Fig. 7. Unfortunately, experimental data for NO_2 are so far unavailable. Nevertheless, it interesting to understand the role of the surface in the production of gas-phase NO_2 molecules. This role depends on the gas pressure and the values of some parameters for surface processes that are unknown. We have assumed steric factors K_i^0 equal to one for all additional (as compared to the model of Ref. 12) surface reactions S15–S19 and the activation energies $E_i \simeq 0$, for S15–S18, and $E_{S19} \simeq 2000$ K. For such values of E_i, the inequalities (49) and (50) are satisfied, and the conditions for surface production of NO_2 are most favorable and controlled by reactions S11–S14 for production of $(NO)_S$ and by desorption processes −S15 and −S16. Here we have used for processes S11–S15 the same parameters as in Ref. 12; have assumed $E_{-S16} = 0$, $\nu_{d\,NO}^0 \simeq \nu_{d\,NO_2}^0 \simeq 10^{13}\ s^{-1}$, and $[F] \simeq 10^{16}\ cm^{-2}$; and have carried out calculations for different values of E_{-S15}. It can be seen from Fig. 7 that the relative rate R_w for surface production of gas-phase NO_2 molecules increases with E_{-S15} and can be nearly 1, which means that interaction with the surface can be the main mechanism for NO_2 production.

V. Conclusions

Self-consistent kinetic models combining volume and surface processes are a new step in the numerical modeling of nonequilibrium plasmas in mixtures of molecular gases. The surface kinetic model developed enables one to obtain the dependence of the probabilities γ_M on the relative concentration of gas-phase atoms and to calculate the rates for surface production of gas-phase NO and NO_2 molecules.

An important peculiarity of this model is the small number of required input parameters, only those externally controlled in experiments: R, I, Q, p, initial gas composition, and T_g. This self-consistent approach provides quantitative interpretation of different experiments and an understanding of the role of different processes. It also enables one to estimate or define more accurately some important rate coefficients and parameters. This was achieved here and elsewhere for rate coefficients and parameters determining 1) the surface kinetics of O and N atoms, 2) associative ionization of N_2 molecules from $N_2(A, a')$ metastables, 3) excitation of $N_2(a')$ from $2N_2(v \geq 16)$, 4) deactivation of $N_2(a')$ on walls, 5) chemical reaction $N_2(v \geq 12) + O \rightarrow NO + N$, and 6) V–E resonant exchanges via $N_2(v \geq 12) + N_2^+(X) \rightarrow N_2(v-12) + N_2^+(B)$.

Acknowledgments

This work was supported by a contract with the Portuguese Ministry of Science and Technology under the Program PRAXIS XXI, partly funded by the European Union Program Fond Européen de Dévelopment Régional and by Project N96-05-66300 of the Russian Foundation for Basic Research.

References

[1] Young, C. K., and Boudart, M., "Recombination of O, N and H on Silica: Kinetics and Mechanism," *Langmuir*, Vol. 7, No. 12, 1991, pp. 2999–3005.

[2] Scott, C. D., "Catalytic Recombination of Nitrogen and Oxygen on High-Temperature Reusable Surface Insulation," AIAA Paper 80-1477, July 1980.

[3] Seward, W. A., and Jumper, E. J., "Model for Oxygen Recombination on Silicon–Dioxide Surfaces," *Thermophysics and Heat Transfer*, Vol. 5, No. 3, pp. 284–291.

[4] Jumper, E. J., Newman, M., Kitchen, D. R., and Seward, W. A., "Recombination of Nitrogen on Silica-Based, Thermal-Protection-Tile-Like Surfaces," AIAA Paper 93-0477, Jan. 1993.

[5] Wise, H., and Wood, B. J., "Reactive Collisions Between Gas and Surface Atoms," *Advances in Molecular and Atomic Physics*, Vol. 3, No. 1, 1967, pp. 291–353.

[6] Nasuti, F., Barbato, M., and Bruno, C., "Material-Dependent Catalytic Recombination Modeling for Hypersonic Flows," AIAA Paper 93-2840, July 1993.

[7] Kovalev, V. L., Suslov, O. N., and Tirskiy, G. A., "Phenomenological Theory for Heterogeneous Recombination of Partially Dissociated Air on High-Temperature Surfaces," *Molecular Physics and Hypersonic Flows*, NATO ASI Series, Series C, Vol. 482, Kluwer Academic, Dordrecht, The Netherlands, 1995, pp. 193–202.

[8] Swenson, G. R., Mende, S. B., and Clifton, K. S., "Ram Vehicle Glow Spectrum; Implication of NO_2 Recombination Continuum," *Geophysical Research Letters*, Vol. 12, No. 2, 1985, pp. 97–100.

[9] Von Zanh, U., and Murad, E., "Nitrogen Dioxide Emitted from Space Shuttle Surfaces and Shuttle Glow," *Nature*, Vol. 321, May 1986, pp. 147, 148.

[10] De Souza, A. R., Mahlmann, C. M., Muzart, J. H., and Speller, C. V., "Influence of Nitrogen on the Oxygen Dissociation in a DC Discharge," *Journal of Physics D: Applied Physics*, Vol. 26, No. 12, 1993, pp. 2164–2167.

[11] Talsky, A., and Zvonicek, V., "The Influence of Impurities on Wall Recombination Coefficient of Atomic Nitrogen," *Abstracts of the 10th Symposium on Elementary Processes and Chemical Reactions in Low Temperature Plasma*, Inst. of Physics, Comenius Univ., Bratislava, Slovakia, 1994, p. 11.

[12] Gordiets, B., Ferreira, C. M., Nahorny, J., Pagnon, D., Touzeau, M., and Vialle, M., "Surface Kinetics of N and O Atoms in N_2–O_2 Discharges," *Journal of Physics D: Applied Physics*, Vol. 29, No. 4, 1996, pp. 1021–1031.

[13] Gordiets, B., Ferreira, C. M., Guerra, V., Loureiro, J., Nahorny, J., Pagnon, D., Touzeau, M., and Vialle, M., "Kinetic Model of a Low-Pressure N_2–O_2 Flowing Glow Discharge," *IEEE Transactions on Plasma Science*, Vol. 23, No. 4, 1995, pp. 750–768.

[14] Loureiro, J., and Ferreira, C. M., "Coupled Electron Energy and Vibrational Distribution Functions in Stationary N_2 Discharges," *Journal of Physics D: Applied Physics*, Vol. 19, No. 1, 1986, pp. 17–36.

[15] Gousset, G., Ferreira, C. M., Pinheiro, M., Sa, M., Touzeau, M., Vialle, M., and Loureiro, J., "Electron and Heavy-Particle Kinetics in the Low Pressure Oxygen Positive Column," *Journal of Physics D: Applied Physics*, Vol. 24, No. 3, 1991, pp. 290–300.

[16] Gordiets, B. F., Osipov, A. I., and Shelepin, L. A., *Kinetic Processes in Gases and Molecular Lasers*, Gordon and Breach, New York, 1986, pp. 228–230.

[17] Armenise, I., Capitelli, M., Garcia, E., Gorse, C., Lagana, A., and Longo, S., "Deactivation Dynamics of Vibrationally Excited Nitrogen Molecules by Nitrogen Atoms. Effects on Non-Equilibrium Vibrational Distribution and Dissociation Rates of Nitrogen Under Electrical Discharges," *Chemical Physics Letters*, Vol. 200, No. 6, 1992, pp. 597–604.

[18] Lagana, A., and Garsia, E., "Temperature Dependence of N–N_2 Rate Coefficients," *Journal of Physical Chemistry*, Vol. 98, No. 2, 1994, pp. 502–507.

[19] Dmitrieva, I. K., and Zenevich, V. A., "Influence of Vibrational Excitation on Rate Coefficients of Reaction $N_2 + O \rightarrow NO + O$. Theoretical–Informational Approximation," *Chemical Physics*, Vol. 3, No. 8, 1984, pp. 1075–1080 (in Russian).

[20] Wedding, A. B., Borysow, J., and Phelps, A. V., "$N_2(a''^1\Sigma_g^+)$ Metastable Collision Destruction and Rotational Excitation Transfer by N_2," *Journal of Chemical Physics*, Vol. 98, No. 8, 1993, pp. 6227–6234.

[21] Piper, L. G., "Quenching Rate Coefficients for $N_2(a'^1\Sigma_u^-)$," *Journal of Chemical Physics*, Vol. 87, No. 3, 1987, pp. 1625–1629.

[22] Kossyi, I. A., Kostinsky, A. Y., Matveyev, A. A., and Silakov, V. P., "Kinetic Scheme of the Non-Equilibrium Discharge in Nitrogen–Oxygen Mixtures," *Plasma Sources Science and Technology*, Vol. 1, No. 3, 1992, pp. 207–220.

[23] Akishev, Y., Derugin, A., Karalnik, V., Kochetov, I., Napartovich, A., and Trushkin, N., "Experimental Investigation and Numerical Modelling of DC Discharge Under Atmospheric Pressure," *Plasma Physics*, Vol. 20, No. 6, 1994, pp. 571–584 (in Russian).

[24] Piper, L. G., "The Excitation of $N_2(B^3\Pi_g, v = 1\text{–}12)$ in the Reaction Between $N_2(A^3\Sigma_u^+)$ and $N_2(X, v \geq 5)$," *Journal of Chemical Physics*, Vol. 91, No. 2, 1989, pp. 864–873.

[25] Heidner, R. F., Sutton, D. G., and Suchard, S. N., "Kinetic Study of $N_2(B^3\Pi_g, v)$ Quenching by Laser-Induced Fluorescence," *Chemical Physics Letters*, Vol. 37, No. 2, 1976, pp. 243–248.

[26] Gordiets, B. F., Ferreira, C. M., Pinheiro, M., and Ricard, A., "Self-Consistent Kinematic Model of Low-Pressure N_2–H_2 Flowing Discharger: I. Volume Processes," *Plasma Sources Science and Technology*, Vol. 7, No. 3, 1998, pp. 363–378.

[27] Magne, L., Cernogora, G., and Veis, P., "Relaxation of Metastable $N_2(a^1\Pi_g, v' = 0\text{–}2)$ in Nitrogen Afterglow," *Journal of Physics D: Applied Physics*, Vol. 25, No. 3, 1992, pp. 472–476.

[28] Krivonosova, O. E., Losev, S. A., Nalivaiko, V. P., Mukoseev, Y. K., and Shatalov, O. P., "The Recommended Data on the Rate Constants of Chemical Reactions with Molecules Involving N and O Atoms," *Plasma Chemistry*, Vol. 14, Energizdat, Moscow, 1987, pp. 3–31 (in Russian).

[29] McEwan, M. J., and Phillips, L. F., *Chemistry of the Atmosphere*, E. Arnold, Wellington, New Zealand, 1975.

[30] Meyer, J. A., Klosterboer, D. H., and Setser, D. W., "Energy Transfer Reaction of $N_2(A^3\Sigma_u^+)$. IV. Measurement of the Radiative Lifetime and Study of the Interaction with Olefins and Other Molecules," *Journal of Chemical Physics*, Vol. 55, No. 5, 1971, pp. 2084–2091.

[31] Cernogora, G., "Etude des Etats Metastables de l'Azote Atomique dans les Decharges Luminescentes," Ph.D. Thesis, Physics Dept., Univ. de Paris-Sud, Centre Orsay, France, Dec. 1980.

[32]Ferreira, C. M., and Loureiro, J., "Characteristic of High-Frequency and DC Argon Discharges at Low Temperatures: A Comparative Analysis," *Journal of Physics D: Applied Physics*, Vol. 17, No. 7, 1984, pp. 1175–1188.

[33]Black, G., Wise, H., Schechter, S., and Sharpless, R. L., "Measurements of Vibrationally Excited Molecules by Raman Scattering. II. Surface Deactivation of Vibrationally Excited N_2," *Journal of Chemical Physics*, Vol. 60, No. 9, 1974, pp. 3526–3536.

[34]Nahorny, J., Pagnon, D., Touzeau, M., Vialle, M., Gordiets, B., and Ferreira, C. M., "Experimental and Theoretical Investigation of a N_2–O_2 DC Flowing Glow Discharge," *Journal of Physics D: Applied Physics*, Vol. 28, No. 4, 1995, pp. 738–747.

[35]Gousset, G., Panafieu, P., Touzeau, M., and Vialle, M., "Experimental Study of a DC Oxygen Glow Discharge by VUV Absorption Spectroscopy," *Plasma Chemistry Plasma Processing*, Vol. 7, No. 4, 1987, pp. 409–427.

[36]Gousset, G., Touzeau, M., Vialle, M., and Ferreira, C. M., "Kinetic Model of a DC Oxygen Glow Discharge," *Plasma Chemistry Plasma Processing*, Vol. 9, No. 2, 1989, pp. 189–206.

[37]Magne, L., Coitout, H., Cernogora, G., and Gousset, G., "Atomic Oxygen Recombination at the Wall in a Time Afterglow," *Journal de Physique III France*, Vol. 3, Sept. 1993, pp. 1871–1889.

[38]Greaves, J. C., and Linnett, J. W., "Recombination of Atoms at Surfaces, Part 6—Recombination of Oxygen Atoms on Silica from 20°C to 600°C," *Transactions of the Faraday Society*, Vol. 55, 1959, pp. 1355–1361.

[39]Steward, D. A., Chen, Y. K., and Henline, W. D., "Effect of Non-Equilibrium Flow Chemistry and Surface Chemistry on Surface Heating to AFE," AIAA Paper 91-1373, June 1991.

[40]Kolodziej, P., and Stewart, D. A., "Nitrogen Recombination on High-Temperature Reusable Surface Insulation and the Analysis of Its Effect on Surface Catalysis," AIAA Paper 87-1637, June 1987.

[41]Marinelli, W. J., and Campbell, J. P., "Spacecraft Metastable Energy Transfer Studies: Final Report," CR NAS9-17565, Physical Sciences, Inc., Andover, MA, July 1986.

[42]Stewart, D. A., and Rakich, J. V., "Catalytic Surface Effects Experiment on Space Shuttle," AIAA Paper 81-1143, June 1981.

[43]Breen, J., Cibrian, R., Delgass, W. N., Keishmann, N. G., Nordine, P. C., and Rosner, D. E., "Catalysis Study for Space Shuttle Vehicle Thermal Protection Systems," NASA CR-134124, Oct. 1973.

[44]Marshall, T. C., "Molecular Storage and Transfer of Electromagnetic Energy in Gaseous Plasmas," Final Rept. RADC-TDR-63-275 (AD-438419), Rome Air Development Center, Griffiss AFB, New York, April 1964.

[45]Rosner, D. E., and Cibrian, R., "Non-Equilibrium Stagnation Region Aerodynamic Heating of Hypersonic Glide Vehicles," AIAA Paper 74-755, 1974.

[46]Back, R. A., "The Decay of Active Nitrogen at High Temperature," *Canadian Journal of Chemistry*, Vol. 37, No. 7, 1959, pp. 2059–2063.

[47]Kelly, R., and Winkler, C. A., "Kinetics of Decay of Nitrogen Atoms as Determined from Chemical Measurements of Atom Concentrations as a Function of Pressure," *Canadian Journal of Chemistry*, Vol. 37, No. 1, 1959, pp. 62–78.

[48]Flowers, O., and Stewart, D. A., "Catalytic Surface Effects on Contaminated Space Shuttle Tiles in a Dissociated Nitrogen Stream," NASA TM-86770, 1985.

K. Kailasanath
Associate Editor